THE JOURNAL OF PHYSICAL CHEMISTRY B

Article

pubs.acs.org/JPCB

Multistate Mechanism of Lysozyme Denaturation through Synchronous Analysis of Raman Spectra

Lei Xing,[†] Ke Lin,[*,§] Xiaoguo Zhou,[†,‡] Shilin Liu,[*,†] and Yi Luo[*,†,‡]

[†]Hefei National Laboratory for Physical Sciences at the Microscale, iChEM (Collaborative Innovation Center of Chemistry for Energy Materials), Department of Chemical Physics and [‡]Synergetic Innovation Center of Quantum Information and Quantum Physics, University of Science and Technology of China, Hefei, Anhui 230026, China

[§]School of Physics and Optoelectronic Engineering, Xidian University, Xi'an, Shanxi 710071, China

ABSTRACT: The denaturation mechanism of hen egg lysozyme is still controversial. In this study, Raman spectroscopy was employed to study the thermal and chemical denaturation mechanisms of lysozyme. All of the Raman bands were synchronously recorded and analyzed during the denaturation process. It was found that the Raman bands of the side groups changed before the bands of skeleton groups. This directly reveals the three-state mechanism of thermal denaturation of lysozyme. The preferential change of the side groups was also observed in the chemical denaturation of lysozyme by guanidine hydrochloride. Moreover, it was found that the Raman bands of the groups on the surface of lysozyme changed before those of the other groups. This indicates that the chemical denaturants interact with the protein surface before the protein core in each step and the chemical denaturation of lysozyme conforms to the multistate and outside-in mechanisms. The synchronous Raman study not only reveals the multistate mechanism of lysozyme denaturation but also demonstrates that this synchronous Raman analysis is a powerful method to study the denaturation mechanisms of other proteins.

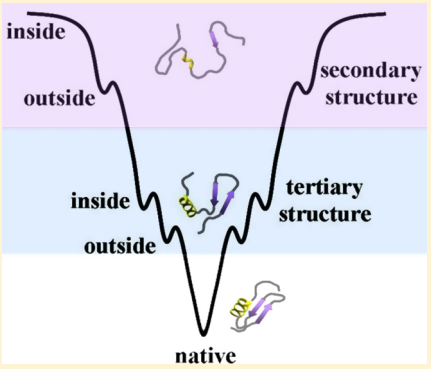

INTRODUCTION

Protein unfolding is important in biological processes.[1−3] It induces some diseases, such as Parkinson's disease or Alzheimer's disease.[4−7] Protein unfolding is described as two-state and multistate transitions.[8,9] The former has an "all-or-none" unfolding manner without any intermediates. The latter involves some stable intermediates in the unfolding process. The absence or presence of any stable intermediate is the key point to differentiate them. To this end, two or more independent probes are recorded during an unfolding transition, as shown in the Scheme 1. If such different probes provide identical transition curves (Scheme 1a), the unfolding follows the two-state model.[10−12] If not (Scheme 1b), the process is multistate.[11,12] The unfolding processes of small globular proteins are usually modeled as two-state transitions.[13,14] Large proteins follow multistate denaturation processes because of the anisotropy of proteins.[15]

Scheme 1. Use of Different Probes to Distinguish Two-State and Multistate Models

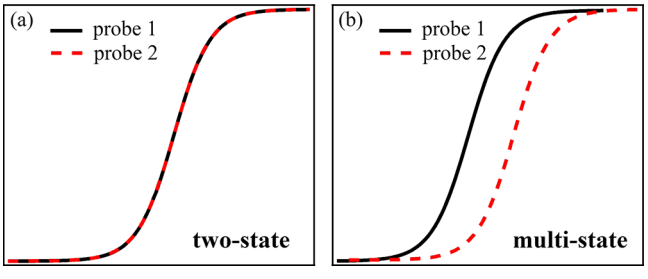

Hen egg lysozyme is a small protein with only 129 amino acids. Previously, the unfolding of lysozyme was considered to be a two-state process. The mechanism was supported by many technologies, such as differential scanning calorimetry,[16,17] liquid chromatography,[18] fluorescence spectroscopy,[19] and Fourier transform infrared (FTIR) spectroscopy.[17] These experimental data were analyzed with a two-state transition.[17,20] However, recently, the two-state model has been challenged by the three-state mechanism through many technologies, such as FTIR spectroscopy,[21] small-angle X-ray spectroscopy,[22] Raman spectroscopy,[23] and molecular dynamics (MD) simulation.[24] A molten globular intermediate was obtained in the three-state process. It was regarded as a molecule with a native-like secondary structure and elastic tertiary structure. However, the evidence for the intermediate was doubted.[25] A particular multistate model called the outside-in action was proposed to explain the chemical denaturation by MD simulations.[24,26,27] The outside-in action means the chemical denaturants first interact with the surface of protein. Very recently, the mechanism was proved by kinetic fluorescence resonance energy transfer and far-UV circular dichroism (CD) spectroscopy,[28] and there has been no equilibrium experimental

Received: August 4, 2016
Revised: September 19, 2016
Published: September 21, 2016

DOI: 10.1021/acs.jpcb.6b07900
J. Phys. Chem. B 2016, 120, 10660−10667

evidence. In a word, the precise mechanism of lysozyme unfolding is still controversial.

Raman spectroscopy is a powerful technology to study protein denaturation. The frequencies, intensities, and bandwidths of Raman bands are sensitive to the structure and microenvironments of a protein. Previously, the vibrational bands of amides I, II, and III were usually used to characterize the secondary structure.[29−32] Recently, the H/D isotopic exchange on the amide I band combined with the low-frequency Raman spectra (LFRS) was employed to study the thermal and chemical denaturation of lysozyme. The results suggested that the amide I band of protein in heavy water and the LFRS were sensitive to the changes in the tertiary structure.[23,33−35] Except the Raman band of amide I and the LFRS, the vibrational bands of the side groups were rarely applied to study the conformational change of proteins in denaturation. Recently, the Raman study on the hydration process of solid lysozyme revealed that the molecular vibration of side groups could offer more information than that of amide groups.[36] Because the molecular interactions between the side groups can stabilize the tertiary structure of protein, the Raman spectra of the side groups may reflect the change of the tertiary structure. To capture the possible intermediate with the elastic tertiary structure and native-like secondary structure, the Raman spectra of the side groups and backbones should be synchronously monitored and analyzed.

In this study, we recorded simultaneously the Raman spectra of the molecular skeletons and the side groups during the thermal and chemical denaturation process of aqueous lysozyme. It was found that the unfolding curves were different between the Raman bands of the side groups and skeleton groups. The difference directly demonstrated the three-state mechanism of thermal denaturation. Furthermore, in the chemical denaturation, the Raman bands of the groups on the surface of lysozyme were found to change preferentially, providing directly equilibrium evidence for the outside-in action of denaturants.

EXPERIMENTAL SECTION

Chicken egg white lysozyme (activity: 22 800 U/mg) and guanidine hydrochloride (GuHCl, 99%) were purchased from Sangon Biotech (Shanghai) Co. Ltd. and Sinopharm Chemical Reagent Co. Ltd., respectively. They were used without further purification. In the thermal denaturation experiment, the weight concentration of lysozyme in water was 10%, which is similar to that in previous Raman studies.[23] The aqueous lysozyme was held in a cuboid quartz cell (1 mm × 1 mm × 3 mm). It was heated from 25 to 85 °C with an interval of 5 or 2 °C through a heating bath (THD-2006; Ningbo). In the mixtures of aqueous lysozyme and GuHCl, the weight concentration of lysozyme was maintained at 17% and the weight concentration of GuHCl was changed from 5 to 44% with an interval of 2 or 1%. The aqueous GuHCl solutions with the corresponding concentrations were prepared to remove the spectral component of GuHCl from the spectra of mixtures. The temperature of the GuHCl solutions was maintained at 25 °C.

The experimental setup is same as that in our previous Raman studies.[37−41] We simply described it here. Spontaneous Raman spectroscopy was used in this study. The backscattering geometry was employed. A continuous-wave laser (532 nm, Verdi V5; Coherent) with 1 W power was employed to excite the aqueous solutions. The laser was linearly polarized through a Glan-laser prism. Parallel polarization of the laser was obtained through a half-wave plate. The Raman scattering light with parallel polarization was selected through a Glan-laser prism and then depolarized through a scrambler. The scattering light was dispersed through a triple monochromator (TriplePro; Acton Research) and then recorded through a liquid-nitrogen-cooled charge-coupled device detector (Spec-10:100B; Princeton Instruments). The wavelength of the scattering light was calibrated through the standard spectral lines of mercury lamp. The resolution of the spectra is about 1−2 cm^{-1}. The acquisition time of the spectra at a single temperature was about 30−40 min, and the spectra were same at the same temperature.

The Raman shifts and the full width at half-maximum (FWHM) of the Raman bands were obtained through fitting the bands with the Lorentzian function.[40] The temperature- or concentration-dependent Raman shifts and FWHM were fitted with a sigmoid function, shown as eq 1.[21,23]

$$S = S_D + \frac{S_N - S_D}{1 + \exp[(B - B_m)/\Delta B]} \quad (1)$$

In this equation, S_N and S_D are the spectral parameters (the Raman shift or FWHM) of the Raman bands of the native and denatured lysozyme, respectively; B denotes the temperature or the concentration of GuHCl; B_m is the transition midpoint of the sigmoid curve; and ΔB denotes half of the transition interval.

RESULTS AND DISCUSSION

Raman Spectra of Lysozyme. Raman spectra of lysozyme were recorded in the region from 400 to 1800 cm^{-1} and 2800 to 3030 cm^{-1}. For clarity, Figure 1 shows the spectra of

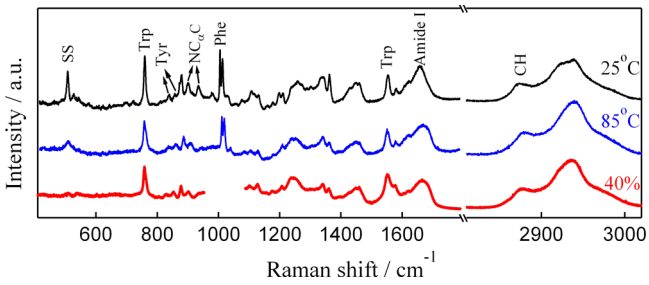

Figure 1. Raman spectra of lysozyme in water at 25 °C (black) and 85 °C (blue) and in aqueous GuHCl with the weight concentration of 40% at 25 °C (red).

lysozyme only in water at 25 and 85 °C and in aqueous GuHCl with the concentration of 40% (m/m) at 25 °C. From the spectra of lysozyme/GuHCl/water, the spectra of GuHCl are removed. The spectra of lysozyme/GuHCl/water around 1000 cm^{-1} are not plotted in Figure 1 because the strong band of GuHCl is difficult to be removed in this region. The Raman bands in the regions from 1030 to 1500 cm^{-1} and above 2900 cm^{-1} are not analyzed quantitatively because these bands are extremely overlapped with each other. Other bands are used to analyze quantitatively the denaturation of lysozyme. They are classified into vibrational bands of skeletons and side groups of lysozyme.

Skeletons. In Figure 1, the band at ∼507 cm^{-1} is assigned to the stretching vibration of disulfide (SS) bridges.[42,43] This band is sensitive to the conformation of the SS bond. The two bands at 900 and 935 cm^{-1} are assigned to the $NC_\alpha C$ stretching

DOI: 10.1021/acs.jpcb.6b07900
J. Phys. Chem. B 2016, 120, 10660−10667

Table 1. Parameters and the Assignments of Raman Bands of Lysozyme

groups	freq. (cm^{-1})	assignment	parameter
skeletons			
SS	507	ν(S−S)[42,43]	FWHM
$NC_\alpha C$	900	ν(N−C_α−C)[44−46]	FWHM
$NC_\alpha C$	935	ν(N−C_α−C) (α-helix)[36,43,44]	frequency
amide	1658	amide I mode[44,47]	frequency
side groups			
Trp	759	symmetric benzene/pyrrole in-phase[46,48]	FWHM
Trp	1554	ν(C_2=C_3)[36,49]	frequency
Tyr	837/857	doublet of the Fermi resonance[a36,50]	frequency
Phe	1005	benzene ring breathing[43,44]	FWHM
C−H	2874	ν(C−H)[51]	frequency

[a]Fermi resonance between the ring breathing mode and overtone of out-of-plane ring deformation.

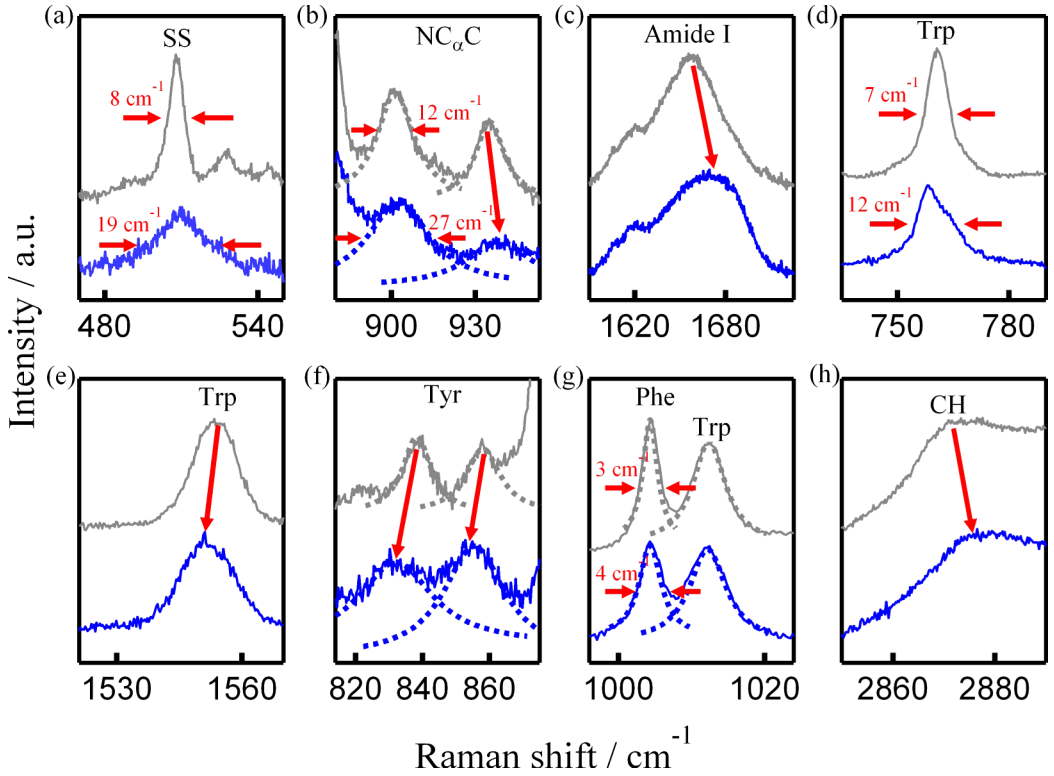

Figure 2. Raman spectra of the SS (a), $NC_\alpha C$ (b), amide I (c), Trp (d, e), Tyr (f), Phe (g), and CH (h) groups of lysozyme at native (25 °C, gray) and denatured (85 °C, blue) states.

vibrations.[36,43−46] Both bands are sensitive to the conformation of $NC_\alpha C$. The band in the 1600−1700 cm^{-1} region is regarded as amide I mode, which is the coupling mode of the C=O and C−N stretching vibration and a small amount of N−H in-plane bending vibration.[44,47] The amide I band (1658 cm^{-1}) is sensitive to the secondary structure of proteins. The frequency of the amide I vibration of α-helix is usually smaller than that of random coil and β-sheet structures.[36,44] The SS stretching band, amide I band, and both $NC_\alpha C$ stretching Raman bands are the vibrations of the skeletons of proteins. They are widely employed to study the skeleton conformation of proteins. In this study, they are employed to quantitatively monitor the structural change of skeletons of lysozyme during the thermal and chemical denaturation processes.

Side Groups. The vibrations of aromatic groups contribute to several Raman bands in Figure 1. The Raman band at 759 cm^{-1} is assigned as the benzene and pyrrole in-phase breathing vibration of tryptophan (Trp).[46,48] The band at 1554 cm^{-1} is attributed to the C_2=C_3 stretching vibration of the aromatic ring of Trp.[36,49] The bands at 837 and 857 cm^{-1} are attributed to the doublet of the Fermi resonance between the ring breathing mode and the overtone of the out-of-plane ring deformation of tyrosine (Tyr).[36,50] The band at 1005 cm^{-1} is assigned to the benzene ring breathing mode of phenylalanine (Phe).[43,44] Besides these vibrational modes of aromatic groups, the CH stretching band at 2874 cm^{-1} is also the vibrational mode of the side groups.[51] The changes in these Raman bands could be employed to monitor the change in the micro-environment around these side groups, which may reflect the change in the tertiary structure of proteins.

The Raman shift and the FWHM of the above Raman bands are employed to quantitatively analyze the structural change of proteins,[36] which are listed in Table 1.

DOI: 10.1021/acs.jpcb.6b07900
J. Phys. Chem. B 2016, 120, 10660−10667

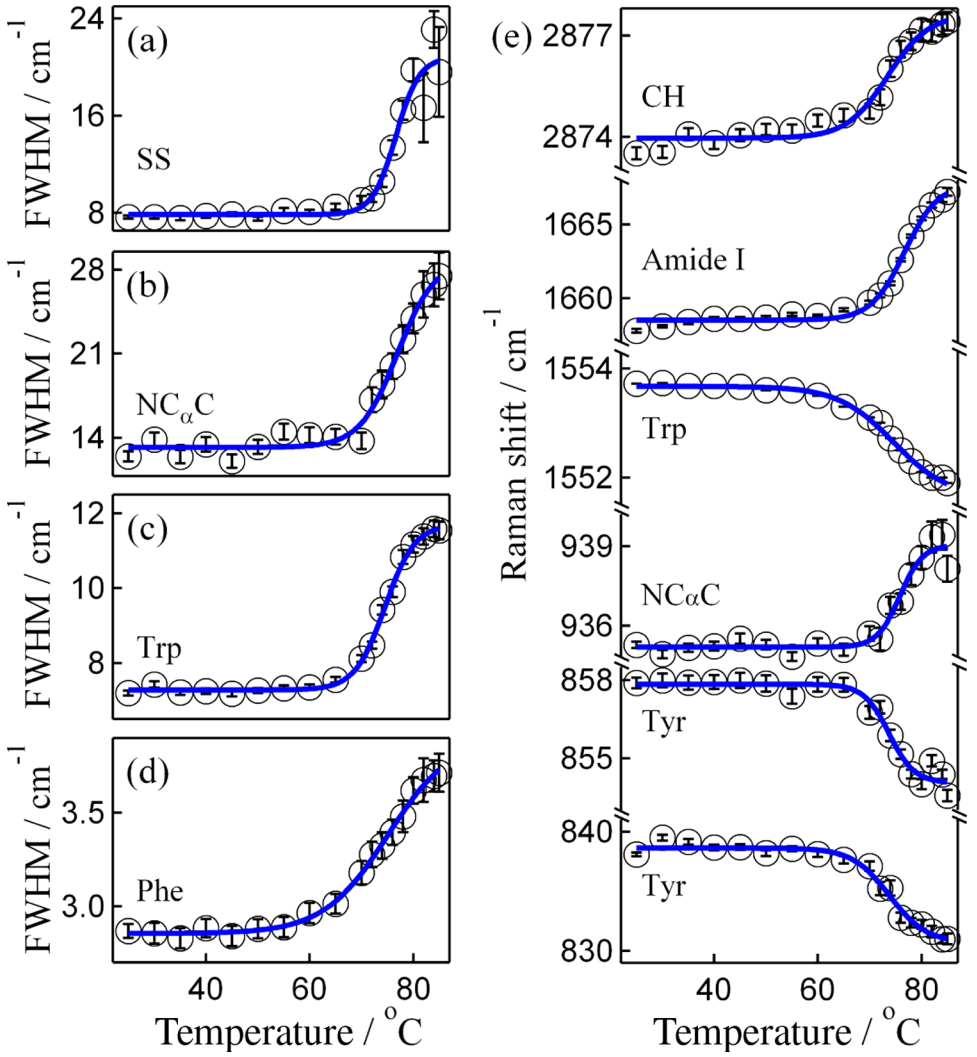

Figure 3. (a) Temperature-dependent FWHM of the Raman bands for SS stretching vibration, (b) N−C_α−C stretching vibration, (c) benzene and pyrrole in-phase breathing vibration of Trp, and (d) benzene ring breathing vibration of Phe; (e) the temperature-dependent Raman shifts of the Raman bands for CH stretching vibration, amide I mode, C_2═C_3 stretching vibration of Trp, N−C_α−C stretching vibration, and the Fermi Resonance doublet of Tyr. The sigmoid function was employed to fit these data.

The Raman bands at the native state (25 °C) and the denatured state (85 °C) are shown in Figure 2. Figure 2a−c shows the Raman spectra of skeletons (SS, $NC_\alpha C$, and amide I). Figure 2d−h shows the Raman spectra of side groups (Trp, Tyr, Phe, and CH). As shown in Figure 2a, from the native state to denatured state, the FWHM of the SS stretching band increases from 8 to 19 cm^{-1}. The broadening of this band demonstrates that the conformation of the SS band transforms to a slightly distorted gauche−gauche−gauche structure.[52] The $NC_\alpha C$ stretching modes (900 and 935 cm^{-1})[36,43−46] are sensitive to the secondary structure. As shown in Figure 2b, from the native state to denatured state, the FWHM of the $NC_\alpha C$ stretching band (900 cm^{-1}) increases from 12 to 27 cm^{-1} and the other $NC_\alpha C$ stretching band shifts from 935 to 939 cm^{-1}. The broadening and blue shift of the $NC_\alpha C$ stretching bands indicate a change in the conformation of $NC_\alpha C$ groups.[46] In addition, the amide I band blue-shifts from 1658 to 1667 cm^{-1} (Figure 2c), which suggests that the α-helix structure transforms to random coil or β-sheet.[34,53]

The vibration modes of skeleton groups are sensitive to the secondary structure; however, the vibration modes of the side groups should be more sensitive to the conformation and microenvironments of these groups. As shown in Figure 2d, the FWHM of Trp band increases from 7 to 12 cm^{-1}, whereas lysozyme changes from the native state to the denatured state. The broadening demonstrates that the conformation distributions of Trp groups are wider at the denatured state.[36] The other Trp Raman band red-shifts from 1554 to 1551 cm^{-1} in Figure 2e, which means the dihedral angle of C_2═C_3−C_β−C_α is decreased.[54,55] Meanwhile, when lysozyme is unfolding, the Tyr Fermi resonance doublet red-shift from 837 to 831 cm^{-1} and 857 to 853 cm^{-1} (Figure 2f) because of the molecular interactions between Tyr and water molecules.[50,56] As shown in Figure 2g, the FWHM of Phe band is increased from 3 to 4 cm^{-1} during the denaturation process. Besides these aromatic vibration modes, the CH band blue-shifts from 2874 to 2877 cm^{-1}, which demonstrates that the CH groups interact with more water at the denatured state.[57,58] As the intermolecular interactions between the side groups stabilize the tertiary structure, the Raman bands of these side groups are applied to monitor the change in the tertiary structures in this study.

Three-State Mechanism of Thermal Denaturation. Figure 3 shows the FWHM and Raman shifts of the above Raman bands at different temperatures. Using the sigmoid

DOI: 10.1021/acs.jpcb.6b07900
J. Phys. Chem. B 2016, 120, 10660−10667

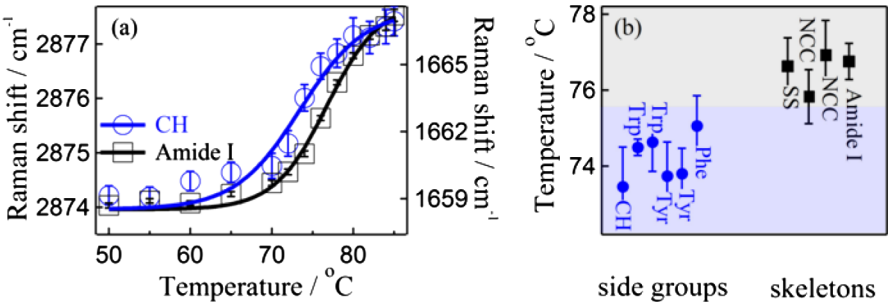

Figure 4. (a) Temperature-dependent Raman shifts of the amide I band (black square) and CH stretching band (blue circle). (b) Midpoint transition temperatures, which are obtained from the temperature-dependent parameters of side groups and skeletons. The error bars in (b) are the fitting errors.

function to fit these data, the midpoint transition temperature (T_m) is obtained to be ~75 °C. This temperature is in agreement with that in previous studies.[17,22,23]

The temperature-dependent Raman shifts and the FWHM of some Raman bands are not identical with each other. For example, the temperature-dependent Raman shifts of amide I band are not synchronous with those of the CH stretching band (Figure 4a). Upon fitting the experimental data with the sigmoid function, the T_m's are determined to be 73.4 ± 1 and 76.8 ± 0.5 °C for CH and amide I groups, respectively. The different T_m values do not conform to the two-state mechanism, as there is only a single T_m in the two-state transition. The lower T_m of CH groups suggests that the microenvironments around CH groups change prior to those around the secondary structure of lysozyme.

Through fitting the temperature-dependent Raman shifts and FWHM of all of the Raman bands with the sigmoid function, 10 midpoint transition temperatures are obtained. These T_m's are plotted in Figure 4b. They are distributed in two different regions. The T_m's from all of the side groups and skeletons of lysozyme are located in the low- (~74 °C) and high-temperature (~76.5 °C) regions, respectively. The Raman bands of side groups are Trp (759, 1554 cm^{-1}), Tyr (837, 857 cm^{-1}), Phe (1005 cm^{-1}), and C−H (2874 cm^{-1}). The Raman bands of skeleton groups are S−S (507 cm^{-1}), N−C_α−C (900, 935 cm^{-1}), and amide I (1658 cm^{-1}). The two-temperature distribution directly indicates that the thermal denaturation of lysozyme follows the three-state mechanism. In the first stage (~74 °C), the microenvironments of the side groups change. The intermolecular interactions between the side groups are weakened, which produces a globular intermediate with a molten tertiary structure.[21−23] In the second stage (~76.5 °C), the skeletons of lysozyme change. A similar two-stage mechanism was also evidenced by the LFRS and H/D isotopic exchange on the amide I band.[23] While the molten tertiary structure was formed, the heavy water molecules penetrated into the core of the proteins and then the H/D isotopic exchange was strengthened. Also because of the molten tertiary structure, the interaction between the protein and solvents was evidenced by the LFRS. The temperature interval between two stages is very small (~2 °C), which may be the reason why a number of previous studies supported the two-state mechanism of thermal denaturation of lysozyme.[16−20]

Multistate and Outside-In Mechanism of Chemical Denaturation. There is also a controversy about the mechanism of chemical denaturation of lysozyme. Both the two-state[59] and multistate[24,60,61] models were supported in previous studies. The synchronous analysis of various Raman bands is also employed to investigate the mechanism of the chemical denaturation of lysozyme with GuHCl in this study. Figure 5 shows the Raman shifts or the FWHM of some Raman

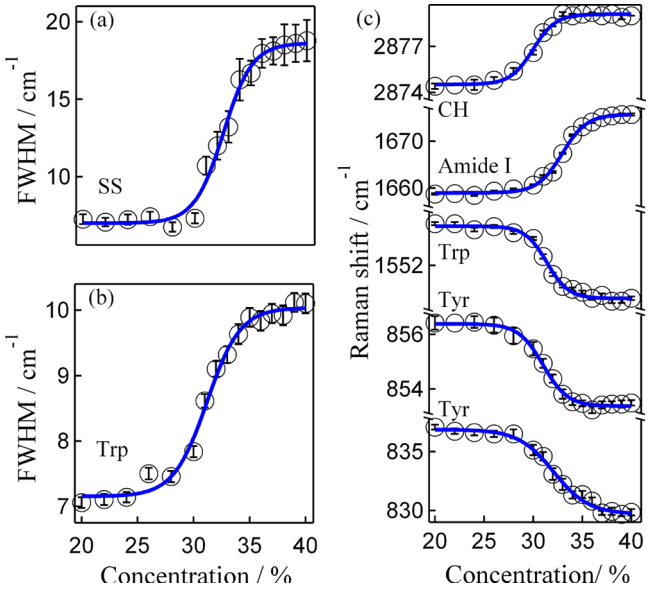

Figure 5. (a) Concentration-dependent FWHM of the Raman bands for SS stretching vibration and (b) the benzene/pyrrole breathing vibration of the Trp group; (c) the concentration-dependent Raman shifts of the Raman bands for CH stretching vibration, amide I mode, C_2═C_3 stretching vibration of Trp, and the Fermi resonance doublet of Tyr. The sigmoid function was employed to fit these data.

bands of lysozyme at different concentrations of GuHCl. These data were all fitted with the sigmoid function. As the Raman bands of Phe (1005 cm^{-1}) and N−C_α−C (900 and 935 cm^{-1}) are extremely overlapped with the strong Raman band of the guanidine ion, these three bands are not analyzed. As shown in Figure 5, the spectral changes in chemical denaturation are similar to those in thermal denaturation. Therefore, the reasons for these spectral changes are similar to those in thermal denaturation.

Although all of the concentration-dependent spectral parameters obey the sigmoid function, they are not identical with each other. For example, the concentration-dependent Raman shifts of the amide I band are much different from those of the CH stretching band (Figure 6a). The midpoint transition concentrations (C_m's) are 30.5 ± 0.1% and 32.9 ± 0.1% for CH groups and amide I groups, respectively. The different C_m's do not conform to the two-state mechanism with single C_m. The

DOI: 10.1021/acs.jpcb.6b07900
J. Phys. Chem. B 2016, 120, 10660−10667

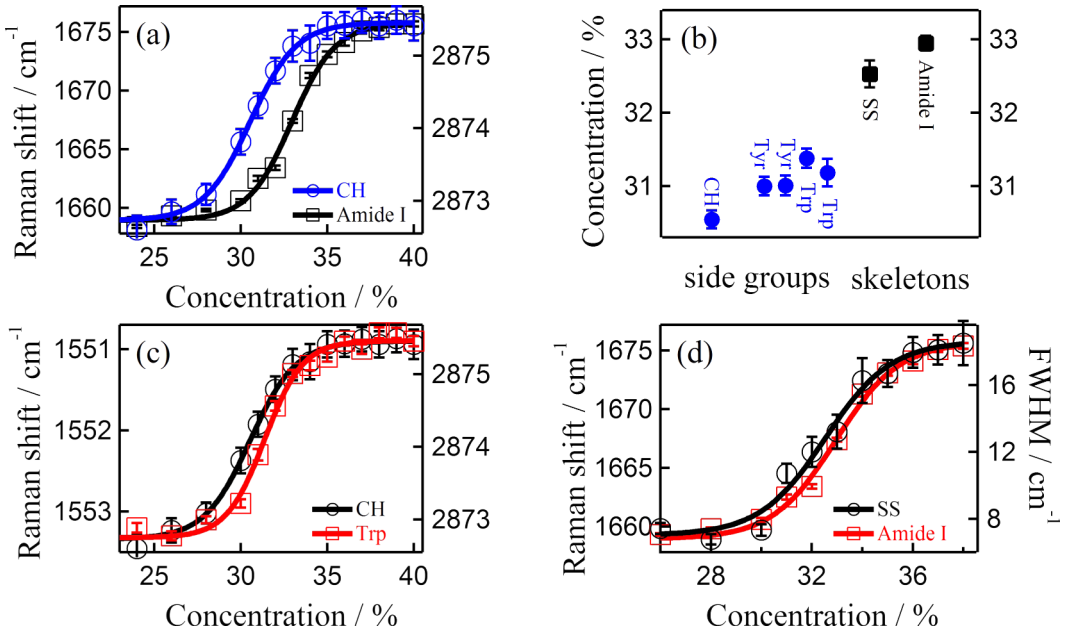

Figure 6. (a) Concentration-dependent Raman shifts of the amide I band (black square) and CH stretching band (blue circle). (b) Midpoint transition concentrations from the Raman bands of side groups and skeletons. (c) Concentration-dependent Raman shifts of the CH stretching band (black cycle) and C_2═C_3 stretching band of the Trp group (red square). (d) Concentration-dependent Raman shifts of the amide I band (red square) and the FWHM of the SS stretching band (black cycle). The error bars in (b) are the fitting errors.

Figure 7. Spatial distribution of the Arg, Lys, Asn, and S−S groups of lysozyme.

lower C_m of CH groups suggests that the microenvironments around CH groups change prior to those around the secondary structure. The C_m's for all of the groups are plotted in Figure 6b. Similar to the T_m distribution of thermal denaturation of lysozyme, the C_m values are distributed roughly in the two concentration regions. The C_m values from all of the side groups (CH, Tyr, and Trp) and skeletons (SS and amide I) of lysozyme are located below and above ∼32%, respectively. This demonstrates that the conformation and microenvironment of side groups change prior to those of the skeleton of lysozyme during chemical denaturation. Furthermore, the C_m values are different from each other in each region. For example, in the low-concentration region (<32%), the CH stretching Raman band changes prior to the C_2═C_3 stretching band of the Trp group (Figure 6c). In the high-concentration region (>32%), the SS stretching band changes prior to the amide I band (Figure 6d). Therefore, the chemical denaturation of lysozyme follows more than two or three states, which fulfills the multistate mechanism.

According to the structure of lysozyme,[62−64] the Arg, Lys, and Asn amino acids are mainly located on the surface of lysozyme (Figure 7). The CH groups of the three amino acids are dominant in all of the CH groups of the amino residues. Consequently, the priority of the change of CH groups in the low-concentration region suggests the preferential interactions between solvents and the surface of lysozyme. Similarly, the SS groups are close to the surface of lysozyme (Figure 7); thus, the priority of the change of SS group in the high-concentration region implies that the skeleton on the surface changes preferentially. Therefore, chemical denaturation of lysozyme obeys the outside-in action. This action was proposed by MD simulations.[24,26,27] According to their description, the outside-in action means the denaturants preferentially interact with the residues on the surface of proteins. This interaction could change the microstructure of the surface of proteins. Then, the change strengthens the penetration of the solvent to the core of proteins. Recently, this outside-in action was also observed in the chemical denaturation process of RNase H protein through the kinetic fluorescence resonance energy transfer and far-UV CD spectroscopy.[28] Similarly, the preferential interactions between the denaturants and the residues on the surface of lysozyme were evidenced by the H/D isotopic exchange on the amide I band and the LFRS.[35] Such as, the hydrogen bonding between the urea and polar groups was limited on the surface of lysozyme. Furthermore, many details of the outside-in action were not observed in previous LFRS. Our Raman spectra offer the direct evidence of the outside-in action of chemical denaturants in equilibrium experiment.

The complete chemical denaturation process of lysozyme can be summarized as the following steps. First, GuHCl interacts with the side groups (such as Arg, Lys, and Asn) on the surface of lysozyme, which induce the change of the conformation and

DOI: 10.1021/acs.jpcb.6b07900
J. Phys. Chem. B 2016, 120, 10660−10667

microenvironments around these exterior side groups. Second, the microenvironments around all of the side groups of lysozyme change when the concentration of GuHCl increases. Both steps refer to the change of the tertiary structure of lysozyme. Third, the skeleton groups (SS) close to the surface of proteins change. Finally, all of the skeleton groups (amide group) of lysozyme change. The final two steps refer to the change in the secondary structure of lysozyme. This complex denaturation behavior demonstrates that the lysozyme with 129 residues is large enough to reflect the anisotropy of this protein. The results suggest that the denaturation of a protein with more residues (such as bull serum albumin[17]) would follow more than two steps.

CONCLUSIONS

The argument about the precise denaturation mechanism of lysozyme has continued for decades. In this study, we synchronously compared the Raman spectra of the side groups and the skeletons during the denaturation of lysozyme. It is found that the Raman spectra of side groups change prior to the spectra of skeletons. This offers the direct evidence to the three-state mechanism of thermal denaturation of lysozyme. In the first stage, the tertiary structure of lysozyme changes. In the second stage, the secondary structure changes. Furthermore, the Raman data offer the direct equilibrium evidence for the theoretical outside-in action[24,26,27] in chemical denaturation by GuHCl. It is found that the surface of lysozyme changes prior to the inside of lysozyme in both the stages, which reflects the multistate mechanism of chemical denaturation of lysozyme. According to the midpoint transition temperatures, the preferential conformational change of CH groups is possible during the first step of the thermal denaturation. However, the outside-in action was not declared because of the larger fitting errors in thermal denaturation. This study not only resolves the dispute about the mechanism of thermal and chemical denaturation of lysozyme but also demonstrates that the synchronous analysis of all of the Raman data is a powerful method to study the denaturation mechanism of proteins.

AUTHOR INFORMATION

Corresponding Authors

*E-mail: klin@xidian.edu.cn. Tel: 18402902609 (K.L.).
*E-mail: slliu@ustc.edu.cn. Tel: 0551-63602323 (S.L.).
*E-mail: yiluo@ustc.edu.cn. Tel: 0551-63607069 (Y.L.).

Notes

The authors declare no competing financial interest.

ACKNOWLEDGMENTS

This research work was supported by the National Natural Science Foundation of China (NSFC, 21473171, 21273211, 21573208), National Key Basic Research Special Foundation (NKBRSF, 2013CB834602), the Chinese Academy of Science, the Fundamental Research Funds for the Central Universities (JB160508), and the Huashan Mountain Scholar Program.

REFERENCES

(1) Matouschek, A. Protein Unfolding-an Important Process in Vivo? *Curr. Opin. Struct. Biol.* **2003**, *13*, 98−109.
(2) Prakash, S.; Matouschek, A. Protein Unfolding in the Cell. *Trends Biochem. Sci.* **2004**, *29*, 593−600.
(3) Eilers, M.; Schatz, G. Protein Unfolding and the Energetics of Protein Translocation across Biological Membranes. *Cell* **1988**, *52*, 481−483.
(4) Dobson, C. M. Principles of Protein Folding, Misfolding and Aggregation. *Semin. Cell Dev. Biol.* **2004**, *15*, 3−16.
(5) Fraser, P. E.; Hawkins, P. N.; Dobson, C. M.; Radfordt, S. E.; Blaket, C. C.; Pepys, M. B. Instability, Unfolding and Aggregation of Human Lysozyme Variants underlying Amyloid Fibrillogenesis. *Nature* **1997**, *385*, 787−793.
(6) Ross, C. A.; Poirier, M. A. Protein Aggregation and Neurodegenerative Disease. *Nat. Med.* **2004**, *10*, S10−17.
(7) Soto, C. Unfolding the Role of Protein Misfolding in Neurodegenerative Diseases. *Nat. Rev. Neurosci.* **2003**, *4*, 49−60.
(8) Eftink, M. R.; Ionescu, R. Thermodynamics of Protein Unfolding: Questions Pertinent to Testing the Validity of the Two-state Model. *Biophys. Chem.* **1997**, *64*, 175−197.
(9) Jha, S. K.; Udgaonkar, J. B. Free Energy Barriers in Protein Folding and Unfolding Reactions. *Curr. Sci.* **2010**, *99*, 457−475.
(10) Streicher, W. W.; Makhatadze, G. I. Calorimetric Evidence for a Two-state Unfolding of the β-hairpin Peptide Trpzip4. *J. Am. Chem. Soc.* **2006**, *128*, 30−31.
(11) Silinski, P.; Allingham, M. J.; Fitzgerald, M. C. Guanidine-induced Equilibrium Unfolding of a Homo-hexameric Enzyme 4-oxalocrotonate Tautomerase (4-OT). *Biochemistry* **2001**, *40*, 4493−4502.
(12) Chedad, A.; Van Dael, H. Kinetics of Folding and Unfolding of Goat α-lactalbumin. *Proteins: Struct., Funct., Bioinf.* **2004**, *57*, 345−356.
(13) Privalov, P. L. Stability of Proteins: Small Globular Proteins. *Adv. Protein Chem.* **1979**, *33*, 167.
(14) Creighton, T. E. Protein Folding. *Biochem. J.* **1990**, *270*, 1.
(15) Anfinsen, C. Principles that Govern the Protein Folding Chains. *Science* **1973**, *181*, 223−230.
(16) Khechinashvili, N.; Privalov, P.; Tiktopulo, E. Calorimetric Investigation of Lysozyme Thermal Denaturation. *FEBS Lett.* **1973**, *30*, 57−60.
(17) Luo, J. J.; Wu, F. G.; Yu, J. S.; Wang, R.; Yu, Z. W. Denaturation Behaviors of Two-State and Non-Two-State Proteins Examined by an Interruption−Incubation Protocol. *J. Phys. Chem. B* **2011**, *115*, 8901−8909.
(18) Uversky, V. N. Use of Fast Protein Size-exclusion Liquid Chromatography to Study the Unfolding of Proteins which Denature through the Molten Globule. *Biochemistry* **1993**, *32*, 13288−13298.
(19) Ibarra-Molero, B.; Sanchez-Ruiz, J. M. Are There Equilibrium Intermediate States in the Urea-induced Unfolding of Hen Egg-white Lysozyme? *Biochemistry* **1997**, *36*, 9616−9624.
(20) Spinozzi, F.; Ortore, M. G.; Sinibaldi, R.; Mariani, P.; Esposito, A.; Cinelli, S.; Onori, G. Microcalorimetric Study of Thermal Unfolding of Lysozyme in Water/Glycerol Mixtures: an Analysis by Solvent Exchange Model. *J. Chem. Phys.* **2008**, *129*, No. 035101.
(21) Van Stokkum, I.; Linsdell, H.; Hadden, J.; Haris, P.; Chapman, D.; Bloemendal, M. Temperature-induced Changes in Protein Structures Studied by Fourier Transform Infrared Spectroscopy and Global Analysis. *Biochemistry* **1995**, *34*, 10508−10518.
(22) Hirai, M.; Arai, S.; Iwase, H. Complementary Analysis of Thermal Transition Multiplicity of Hen Egg-white Lysozyme at Low pH Using X-ray Scattering and Scanning Calorimetry. *J. Phys. Chem. B* **1999**, *103*, 549−556.
(23) Hédoux, A.; Ionov, R.; Willart, J. F.; Lerbret, A.; Affouard, F.; Guinet, Y.; Descamps, M.; Prevost, D.; Paccou, L.; Danede, F. Evidence of a Two-stage Thermal Denaturation Process in Lysozyme: a Raman Scattering and Differential Scanning Calorimetry Investigation. *J. Chem. Phys.* **2006**, *124*, No. 014703.
(24) Hua, L.; Zhou, R.; Thirumalai, D.; Berne, B. Urea Denaturation by Stronger Dispersion Interactions with Proteins than Water Implies a 2-stage Unfolding. *Proc. Natl. Acad. Sci. U.S.A.* **2008**, *105*, 16928−16933.
(25) Meersman, F.; Heremans, K. Temperature-induced Dissociation of Protein Aggregates: Accessing the Denatured State. *Biochemistry* **2003**, *42*, 14234−14241.
(26) Wallqvist, A.; Covell, D.; Thirumalai, D. Hydrophobic Interactions in Aqueous Urea Solutions with Implications for the

DOI: 10.1021/acs.jpcb.6b07900
J. Phys. Chem. B 2016, 120, 10660−10667

Mechanism of Protein Denaturation. *J. Am. Chem. Soc.* **1998**, *120*, 427−428.
(27) Mountain, R. D.; Thirumalai, D. Molecular Dynamics Simulations of End-to-end Contact Formation in Hydrocarbon Chains in Water and Aqueous Urea Solution. *J. Am. Chem. Soc.* **2003**, *125*, 1950−1957.
(28) Jha, S. K.; Marqusee, S. Kinetic Evidence for a Two-stage Mechanism of Protein Denaturation by Guanidinium Chloride. *Proc. Natl. Acad. Sci. U.S.A.* **2014**, *111*, 4856−4861.
(29) Alix, A.; Pedanou, G.; Berjot, M. Fast Determination of the Quantitative Secondary Structure of Proteins by Using Some Parameters of the Raman Amide I Band. *J. Mol. Struct.* **1988**, *174*, 159−164.
(30) Byler, D. M.; Susi, H. Examination of the Secondary Structure of Proteins by Deconvolved FTIR Spectra. *Biopolymers* **1986**, *25*, 469−487.
(31) Kong, J.; Yu, S. Fourier Transform Infrared Spectroscopic Analysis of Protein Secondary Structures. *Acta Biochim. Biophys. Sin.* **2007**, *39*, 549−559.
(32) Tinti, A.; Di Foggia, M.; Taddei, P.; Torreggiani, A.; Dettin, M.; Fagnano, C. Vibrational Study of Auto-assembling Oligopeptides for Biomedical Applications. *J. Raman Spectrosc.* **2008**, *39*, 250−259.
(33) Hédoux, A.; Willart, J.; Ionov, R.; Affouard, F.; Guinet, Y.; Paccou, L.; Lerbret, A.; Descamps, M. Analysis of Sugar Bioprotective Mechanisms on the Thermal Denaturation of Lysozyme from Raman Scattering and Differential Scanning Calorimetry Investigations. *J. Phys. Chem. B* **2006**, *110*, 22886−22893.
(34) Seo, J. A.; Hédoux, A.; Guinet, Y.; Paccou, L.; Affouard, F.; Lerbret, A.; Descamps, M. Thermal Denaturation of Beta-lactoglobulin and Stabilization Mechanism by Trehalose Analyzed from Raman Spectroscopy Investigations. *J. Phys. Chem. B* **2010**, *114*, 6675−6684.
(35) Hédoux, A.; Krenzlin, S.; Paccou, L.; Guinet, Y.; Flament, M.-P.; Siepmann, J. Influence of Urea and Guanidine Hydrochloride on Lysozyme Stability and Thermal Denaturation; a Correlation between Activity, Protein Dynamics and Conformational Changes. *Phys. Chem. Chem. Phys.* **2010**, *12*, 13189−13196.
(36) Kocherbitov, V.; Latynis, J.; Misiu-nas, A.; Barauskas, J.; Niaura, G. Hydration of Lysozyme Studied by Raman Spectroscopy. *J. Phys. Chem. B* **2013**, *117*, 4981−4992.
(37) Chen, L.; Zhu, W.; Lin, K.; Hu, N.; Yu, Y.; Zhou, X.; Yuan, L. F.; Hu, S. M.; Luo, Y. Identification of Alcohol Conformers by Raman Spectra in the C−H Stretching Region. *J. Phys. Chem. A* **2015**, *119*, 3209−3217.
(38) Lin, K.; Zhou, X.; Luo, Y.; Liu, S. The Microscopic Structure of Liquid Methanol from Raman Spectroscopy. *J. Phys. Chem. B* **2010**, *114*, 3567−3573.
(39) Lin, K.; Zhou, X. g.; Liu, S. l.; Luo, Y. Identification of Free OH and Its Implication on Structural Changes of Liquid Water. *Chin. J. Chem. Phys.* **2013**, *26*, 121−127.
(40) Lin, K.; Hu, N.; Zhou, X.; Liu, S.; Luo, Y. Reorientation Dynamics in Liquid Alcohols from Raman Spectroscopy. *J. Raman Spectrosc.* **2012**, *43*, 82−88.
(41) Tang, C. Q.; Lin, K.; Zhou, X. G.; Liu, S. L. In situ Detection of Amide A Bands of Proteins in Water by Raman Ratio Spectrum†. *Chin. J. Chem. Phys.* **2016**, *29*, 129−134.
(42) Sugeta, H.; Go, A.; Miyazawa, T. Vibrational Spectra and Molecular Conformations of Dialkyl Disulfides. *Bull. Chem. Soc. Jpn.* **1973**, *46*, 3407−11.
(43) Wen, Z. Q. Raman Spectroscopy of Protein Pharmaceuticals. *J. Pharm. Sci.* **2007**, *96*, 2861−2878.
(44) Spiro, T. G.; Gaber, B. P. Laser Raman Scattering as a Probe of Protein Structure. *Annu. Rev. Biochem.* **1977**, *46*, 553−570.
(45) Lord, R.; Yu, N. T. Laser-excited Raman Spectroscopy of Biomolecules: I. Native Lysozyme and Its Constituent Amino Acids. *J. Mol. Struct.* **1970**, *50*, 509−524.
(46) Chen, M.; Lord, R.; Mendelsohn, R. Laser-excited Raman Spectroscopy of Biomolecules. V. Conformational Changes Associated with the Chemical Denaturation of Lysozyme. *J. Am. Chem. Soc.* **1974**, *96*, 3038−3042.
(47) Ellis, D. I.; Cowcher, D. P.; Ashton, L.; O'Hagan, S.; Goodacre, R. Illuminating Disease and Enlightening Biomedicine: Raman Spectroscopy as a Diagnostic Tool. *Analyst* **2013**, *138*, 3871.
(48) Sweeney, J. A.; Asher, S. A. Tryptophan UV resonance Raman Excitation Profiles. *J. Phys. Chem.* **1990**, *94*, 4784−4791.
(49) Rygula, A.; Majzner, K.; Marzec, K.; Kaczor, A.; Pilarczyk, M.; Baranska, M. Raman Spectroscopy of Proteins: a Review. *J. Raman Spectrosc.* **2013**, *44*, 1061−1076.
(50) Siamwiza, M. N.; Lord, R. C.; Chen, M. C.; Takamatsu, T.; Harada, I.; Matsuura, H.; Shimanouchi, T. Interpretation of the Doublet at 850 and 830 cm^{-1} in the Raman Spectra of Tyrosyl Residues in Proteins and Certain Model Compounds. *Biochemistry* **1975**, *14*, 4870−4876.
(51) Howell, N. K.; Arteaga, G.; Nakai, S.; Li-Chan, E. C. Raman Spectral Analysis in the CH Stretching Region of Proteins and Amino Acids for Investigation of Hydrophobic Interactions. *J. Agric. Food Chem.* **1999**, *47*, 924−933.
(52) Hédoux, A.; Guinet, Y.; Paccou, L. Analysis of the Mechanism of Lysozyme Pressure Denaturation from Raman Spectroscopy Investigations, and Comparison with Thermal Denaturation. *J. Phys. Chem. B* **2011**, *115*, 6740−6748.
(53) Torreggiani, A.; Di Foggia, M.; Manco, I.; De Maio, A.; Markarian, S.; Bonora, S. Effect of Sulfoxides on the Thermal Denaturation of Hen lysozyme: a Calorimetric and Raman Study. *J. Mol. Struct.* **2008**, *891*, 115−122.
(54) Takeuchi, H. UV Raman Markers for Structural Analysis of Aromatic Side Chains in Proteins. *Anal. Sci.* **2011**, *27*, 1077.
(55) Takeuchi, H. Raman Structural Markers of Tryptophan and Histidine Side Chains in Proteins. *Biopolymers* **2003**, *72*, 305−317.
(56) Chen, M.; Lord, R.; Mendelsohn, R. Laser-excited Raman Spectroscopy of Biomolecules: IV. Thermal Denaturation of Aqueous Lysozyme. *Biochim. Biophys. Acta, Protein Struct.* **1973**, *328*, 252−260.
(57) Qian, W.; Krimm, S. Vibrational Spectroscopy of Hydrogen Bonding: Origin of the Different Behavior of the CH···O Hydrogen Bond. *J. Phys. Chem. A* **2002**, *106*, 6628−6636.
(58) Scheiner, S.; Kar, T. Effect of Solvent upon CH···O Hydrogen Bonds with Implications for Protein Folding. *J. Phys. Chem. B* **2005**, *109*, 3681−3689.
(59) Greene, R. F.; Pace, C. N. Urea and Guanidine Hydrochloride Denaturation of Ribonuclease, Lysozyme, α-chymotrypsin, and β-lactoglobulin. *J. Biol. Chem.* **1974**, *249*, 5388−5393.
(60) Laurents, D.; Baldwin, R. Characterization of the Unfolding Pathway of Hen Egg White Lysozyme. *Biochemistry* **1997**, *36*, 1496−1504.
(61) Sasahara, K.; Demura, M.; Nitta, K. Partially Unfolded Equilibrium State of Hen Lysozyme Studied by Circular Dichroism Spectroscopy. *Biochemistry* **2000**, *39*, 6475−6482.
(62) Chen, C.-D.; Huang, Y.-C.; Chiang, H.-L.; Hsieh, Y.-C.; Guan, H.-H.; Chuankhayan, P.; Chen, C.-J. Direct Phase Selection of Initial Phases From Single-wavelength Anomalous Dispersion (SAD) for the Improvement of Electron Density and Aβ Initio Structure Determination. *Acta Crystallogr., Sect. D: Biol. Crystallogr.* **2014**, *70*, 2331−2343.
(63) Huerta-Viga, A.; Woutersen, S. Protein Denaturation with Guanidinium: A 2D-IR Study. *J. Phys. Chem. Lett.* **2013**, *4*, 3397−3401.
(64) Cha, S.-S.; An, Y. J.; Jeong, C.-S.; Kim, M.-K.; Lee, S.-G.; Lee, K.-H.; Oh, B.-H. Experimental Phasing Using Zinc Anomalous Scattering. *Acta Crystallogr., Sect. D: Biol. Crystallogr.* **2012**, *68*, 1253−1258.

DOI: 10.1021/acs.jpcb.6b07900
J. Phys. Chem. B 2016, 120, 10660−10667